Physica C: Superconductivity and its applications 543 (2017) 46–51

Contents lists available at ScienceDirect

Physica C: Superconductivity and its applications

journal homepage: www.elsevier.com/locate/physc

Fluxoids configurations in finite superconducting networks

Omri J. Sharon, Noam Haham, Avner A. Shaulov, Yosef Yeshurun*

Department of Physics and Institute of Nano Technology and Advanced Materials, Bar-Ilan University, 5290002 Ramat-Gan, Israel

ARTICLE INFO

Article history:
Received 11 May 2017
Revised 7 September 2017
Accepted 12 October 2017
Available online 14 October 2017

ABSTRACT

Analysis of superconducting ladders consisting of rectangular loops, yields an Ising like expression for the total energy of the ladders as a function of the loops vorticities and the applied magnetic field. This expression shows that fluxoids can be treated as repulsively interacting objects driven towards the ladder center by the applied field. Distinctive repulsive interactions between fluxoids are obtained depending on the ratio l between the loops length and the common width of adjacent loops. A 'short range' and a 'long range' interactions obtained for $l \gtrsim 1$ and $l \ll 1$, respectively, give rise to remarkably different fluxoid configurations. The different configurations of fluxoids in different types of ladders are illustrated by simulations.

1. Introduction

Macroscopic quantum phenomena continue to attract attention since the early days of quantum mechanics [1]. A prominent example of a macroscopic quantum phenomenon is exhibited by loops and networks made of thin superconducting wires. The quantity quantized in these multiply-connected systems is the fluxoid defined as: $(4\pi\lambda^2/c)\oint \vec{J}\cdot\vec{dl} + \phi$, where $\vec{J}$ is the density of the shielding current in a loop, λ is the penetration depth, and ϕ is the magnetic flux threading the loop. In each and every loop of a network the fluxoid must be an integer multiple of the flux quantum ϕ_0 [2]. The requirement of minimum energy determines the number and arrangement of fluxoids in the network giving rise to periodic changes in the energy as a function of the external field.

Fluxoid quantization effects have been studied extensively, both theoretically and experimentally, in a variety of superconducting networks [3-17]. However, most of these studies focus on the phase boundary between the superconducting and the normal states, paying less attention to the fluxoids configuration in the networks as a function of the applied magnetic field. The limited number of studies considering fluxoids configurations present results of experimentally measured or theoretically calculated configurations in various networks, providing no intuitive understanding of the underlying physics [6,17-19]. The purpose of the present work is to elucidate the mechanism governing the fluxoid configuration in finite superconducting networks as a function of the applied field. Understanding the physics behind the different fluxoid configurations may lead to the development of new concepts in 'fluxonics' – a growing research area aiming at exploiting superconductors in digital circuits [20-23].

We theoretically analyze the simplest case of a superconducting 1D network ('ladder') using the "current squared" model (known as the "J^2 model") [6,18,24]. In this model the kinetic energy of the network is calculated as the sum of the squared currents over all the network wires, and the number and arrangement of the fluxoids are determined by the requirement of minimum energy. Our analysis yields an Ising like expression for the total energy of the network as a function of the loops' vorticities and the applied magnetic field. This expression shows that fluxoids can be treated as repulsively interacting objects subjected to an additional interaction with the applied field. The field tends to direct the fluxoids towards the network center while fluxoids repel each other tending to keep themselves apart. Competition between these two interactions determines the equilibrium arrangement of fluxoids in the network as a function of the applied field.

We distinguish between three types of ladders depending on the ratio l between the loops' length and the common width of adjacent loops in the ladder. For $l >> 1$, the interaction between fluxoids is negligible and the ladder can essentially be considered as a collection of separate, non-interacting loops. As the ratio l decreases toward 1, 'short range' repulsive interactions arise, decreasing exponentially with the relative positions of the fluxoids. Ladders with $l << 1$ are characterized by a 'long range' interaction, which depends on the product of the fluxoids' locations relative to the ladder's edges. The different configurations of fluxoids in these different types of ladders are illustrated by simulations.

* Corresponding author.
E-mail address: yeshurun@mail.biu.ac.il (Y. Yeshurun).

https://doi.org/10.1016/j.physc.2017.10.007
0921-4534/

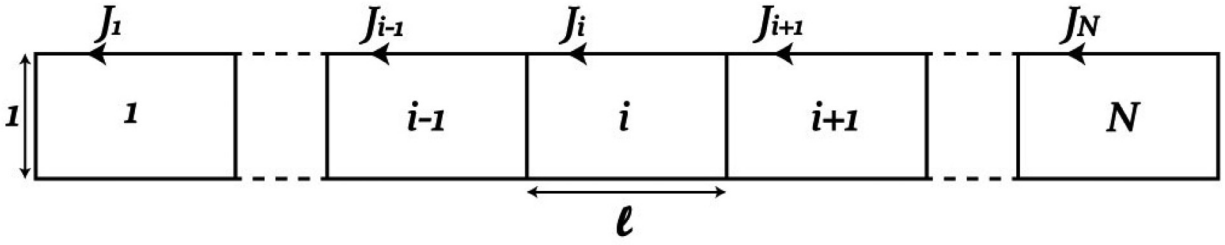

Fig. 1. Finite rectangular ladder consisting of N loops.

2. Analysis

Consider a superconducting ladder of finite length, consisting of N rectangular loops of unit width and length l, as shown in Fig. 1.

The fluxoid quantization equation for loop i reads:

$$2(l+1)J_i - J_{i-1} - J_{i+1} = n_i - \frac{\phi}{\phi_0}, \tag{1}$$

where n_i is the vorticity of the loop i, ϕ is the flux threading this loop, and by definition $J_i = 0$ for $i < 0$ or $i > N$. For simplicity, the coefficient $4\pi\lambda^2/c$ is taken as 1. According to Eq. (1), the set of the fluxoid quantization equations for all the loops can be written as a matrix equation:

$$\hat{A}\cdot\vec{J} = \vec{n} - \frac{\vec{\phi}}{\phi_0}, \tag{2}$$

where the elements of the matrix $\hat{A}$:

$$A_{ij} = 2(l+1)\delta_{i,j} - \delta_{i,j-1} - \delta_{i,j+1},$$

$\delta_{i,j}$ being the Kronecker δ.

The current vector $\vec{J}$ can be calculated from Eq. (2) by inversion:

$$\vec{J} = \hat{A}^{-1}\left(\vec{n} - \frac{\vec{\phi}}{\phi_0}\right) \tag{3}$$

Denoting the matrix $\hat{A}^{-1}$ as $\hat{B}$, Eq. (3) can be written as a set of equations:

$$J_i = \sum_{j=1}^{N} B_{ij}\left(n_j - \frac{\phi}{\phi_0}\right), \quad i = 1..N. \tag{4}$$

Using the J^2 model, knowledge of J_i allows calculation of the energy E_i of the loop i:

$$E_i = 2lJ_i^2 + \frac{1}{2}(J_i - J_{i-1})^2 + \frac{1}{2}(J_i - J_{i+1})^2 + \frac{1}{2}J_1^2\delta_{1,i} + \frac{1}{2}J_N^2\delta_{N,i}$$

$$= J_i[(2l+1)J_i - J_{i-1} - J_{i+1}] + \frac{1}{2}J_{i-1}^2 + \frac{1}{2}J_{i+1}^2 + \frac{1}{2}J_1^2\delta_{1,i} + \frac{1}{2}J_N^2\delta_{N,i},$$

and the total energy E of the network:

$$E = \sum_{i=1}^{N} E_i = \sum_{i=1}^{N}\left\{J_i(-J_i + 2(l+1)J_i - J_{i-1} - J_{i+1}) + \frac{1}{2}J_{i-1}^2 + \frac{1}{2}J_{i+1}^2\right\} + \frac{1}{2}J_1^2 + \frac{1}{2}J_N^2. \tag{5}$$

Using Eq. (1) and realizing that $\sum_{i=1}^{N}\{-J_i^2 + \frac{1}{2}J_{i-1}^2 + \frac{1}{2}J_{i+1}^2\} + \frac{1}{2}J_1^2 + \frac{1}{2}J_N^2 = 0$, Eq. (5) becomes

$$E = \sum_{i=1}^{N} J_i\left(n_i - \frac{\phi}{\phi_0}\right). \tag{6}$$

Inserting J_i from Eq. (4) yields

$$E = \sum_{i=1}^{N}\sum_{j=1}^{N} B_{ij}\left(n_j - \frac{\phi}{\phi_0}\right)\left(n_i - \frac{\phi}{\phi_0}\right) = \sum_{ij} B_{ij}\left(n_i n_j - 2\frac{\phi}{\phi_0}\, n_i + \left(\frac{\phi}{\phi_0}\right)^2\right) \tag{7}$$

The above expression for the total energy, E, is reminiscent of the Ising model for the energy of a spin configuration, having the form $\sum_{ij} J_{ij}S_iS_j - \mu\sum_j h_jS_j$ [25]; n_j, and B_{ij} playing the role of the Ising variable S_j and the exchange energy J_{ij}, respectively. The first term on the right hand side of Eq. (7), $(\sum_{ij} B_{ij}n_in_j)$, represents the interaction between fluxoids, including the self-interactions $\sum_i B_{ii}n_i^2$. The second term $(-2\frac{\phi}{\phi_0}\sum_{ij} n_iB_{ij})$ expresses the interaction between the fluxoids and the effective magnetic field. The third term, $(\frac{\phi}{\phi_0})^2\sum_{ij} B_{ij}$, is a constant, independent of the vorticities and thus may be ignored.

For the matrix $\hat{A}$ given in Eq. (2), $\hat{B} = \hat{A}^{-1}$ is a symmetric matrix with elements [26]:

$$B_{ij} = \frac{\left(\gamma_1^i - \gamma_2^i\right)\left(\gamma_1^{N+1-j} - \gamma_2^{N+1-j}\right)}{(\gamma_1 - \gamma_2)\left(\gamma_1^{N+1} - \gamma_2^{N+1}\right)}, \quad \text{for } i \le j \tag{8}$$

where $\gamma_{1,2} = (l+1) \pm \sqrt{(l+1)^2 - 1}$. Due to the symmetry of $\hat{B}$, B_{ij} for $i > j$ can be calculated as B_{ji} using Eq. (4). Defining $\eta \equiv \gamma_2/\gamma_1$, and $C \equiv 1/(1-\eta)(1-\eta^{N+1})$, Eq. (8) takes the form

$$B_{ij} = C\gamma_1^{i-j-1}\left(1 - \eta^i\right)\left(1 - \eta^{N+1-j}\right), \text{for } i \le j. \tag{9}$$

γ_1, γ_2, η and C are geometrical factors that depend on the element length l. These dependencies are shown in Fig. 2.

As clarified below, l determines the degree of coupling between the loops. For $l \gg 1$, the coupling is weak, and for $l \ll 1$ the coupling is strong. These two cases differ significantly from each other and from the intermediate case $l \gtrsim 1$, on which interest is commonly focused. In the following we discuss these three limiting cases:

Case 1: $l \gg 1$. In this case, $C \to 1$, $\eta \to 0$, and the off-diagonal elements of the matrix $\hat{B}$ become negligible as compared to the diagonal elements. Thus, the dependence of J_i on the vorticities of loops, other than the loop i, can be neglected (see Eq. 4). In other words, the coupling between the loops is weak and the energy of the ladder is approximately the sum of the energies of separate loops:

$$E = \gamma_1^{-1}\sum_{i=1}^{N}\left(n_i^2 - 2\frac{\phi}{\phi_0}\, n_i + \left(\frac{\phi}{\phi_0}\right)^2\right). \tag{10}$$

Consequently, as the field increases, all the loops are occupied with fluxoids essentially in unison.

Case 2: $l \gtrsim 1$. In this case, $\eta \ll 1$, $C \approx 1$ and γ_1 approximately equals to the circumference $2(l+1)$ of a single loop. Thus, it is justified to neglect in Eq. (9) powers of η as compared to 1, and approximate B_{ij} as $\gamma_1^{-(|i-j|+1)}$. In this approximation, Eq. (7) becomes

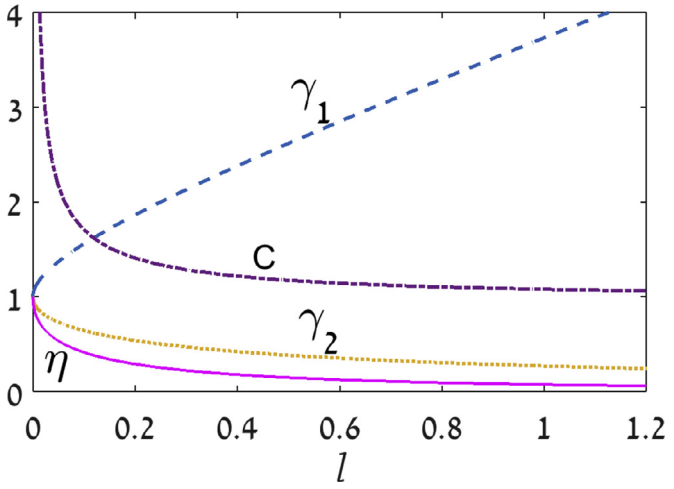

Fig. 2. The geometrical factors γ_1, γ_2, C and η as a function of the ratio l between the loop length and the common width of adjacent loops.

$$E = \sum_{ij} \gamma_1^{-(|i-j|+1)} \left(n_i n_j - 2\frac{\phi}{\phi_0}\, n_i + \left(\frac{\phi}{\phi_0}\right)^2 \right). \tag{11}$$

The above expression shows that fluxoids can be treated as repulsively interacting objects, with interaction energy that decreases exponentially with their separation in the ladder. In order to minimize the total energy, the repulsive interaction between fluxoids tends to keep them away from each other. The interaction between the fluxoids and the effective magnetic field, represented by the second term in Eq. (11), $(-2\frac{\phi}{\phi_0}\sum_i n_i \sum_j \gamma_1^{-(|i-j|+1)})$, reduces the energy depending on the fluxoids arrangement within the network. It can be shown that the geometric progression factor in this term: $-\sum_j \gamma_1^{-(|i-j|+1)} \propto \cosh(\ln(\gamma_1)(\frac{N+1}{2} - i))$, which is minimal at the center of the ladder ($i = \frac{N+1}{2}$). Thus, to minimize the total energy, the interaction with the field, tends to drive the fluxoids away from the network edges towards the network's center. As mentioned above, the third term in Eq. (8), $(\frac{\phi}{\phi_0})^2 \sum_{ij} \gamma_1^{-(|i-j|+1)}$, is independent of the vorticities and thus can be ignored. We conclude that while the external magnetic field tends to assemble the fluxoids near the ladder center, the fluxoids repel each other tending to keep themselves apart. Competition between these two opposite interactions determines the equilibrium arrangement of fluxoids in the network as a function of the applied field. The self-interaction term has no role as it has no spatial preference, because in this case the diagonal elements $B_{ii} = \gamma_1^{-1}$ are all the same. Considering the first fluxoid which enters the ladder, it will always appear at the center of the network (or next to it, in a ladder with an even number of loops) as it is affected only by the external field which drives it to the center. As the field increases, a second fluxoid enters the system, pushing the first one out of its central position and both fluxoids arrange themselves in an optimum configuration, keeping apart from each other and away from the network edges. The same principle determines the arrangements of the next fluxoids entering the ladder as the field further increases. Rearrangement of fluxoids in the network continues until the last fluxoid enters at the network center completing one period in which each loop is occupied with one fluxoid. Occupation of the loops in the following periods follows the same pattern.

Case 3: $l \ll 1$. In this case, both γ_1 and η approach 1 and

$$B_{ij} \to \frac{i(N+1-j)}{N+1} \text{ for } i \le j. \tag{12}$$

Thus, the repulsive interaction between fluxoids becomes dependent on the product of their locations relative to the ladder's edges. This is in variance with the previous case ($l \gtrsim 1$) in which the interaction between fluxoids decreased exponentially with their relative locations. In addition, contrary to the case $l \gtrsim 1$, where the diagonal elements $B_{ii} = \gamma_1^{-1}$ are all the same, independent of the location i, in the case $l \ll 1$, $B_{ii} = i(N+1-i)/(N+1)$ has a maximum value of $(N+1)/4$ at the center of the ladder (i.e. for $i = (N+1)/2$) and drops parabolicaly to $N/(N+1)$ at the ladder's edges ($i = 1$, and $i = N$). Consequently, the fluxoid self-energy,

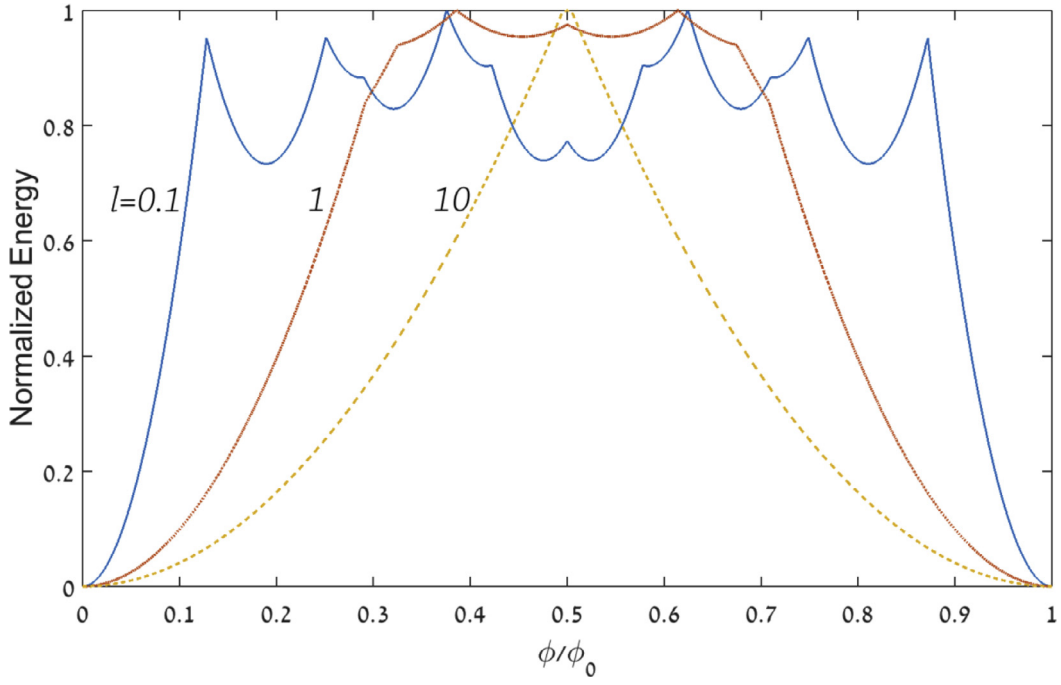

Fig. 3. Normalized energy as a function of the normalized magnetic flux in ladders with 11 loops and different ratios l between the loop length and the common width of adjacent loops.

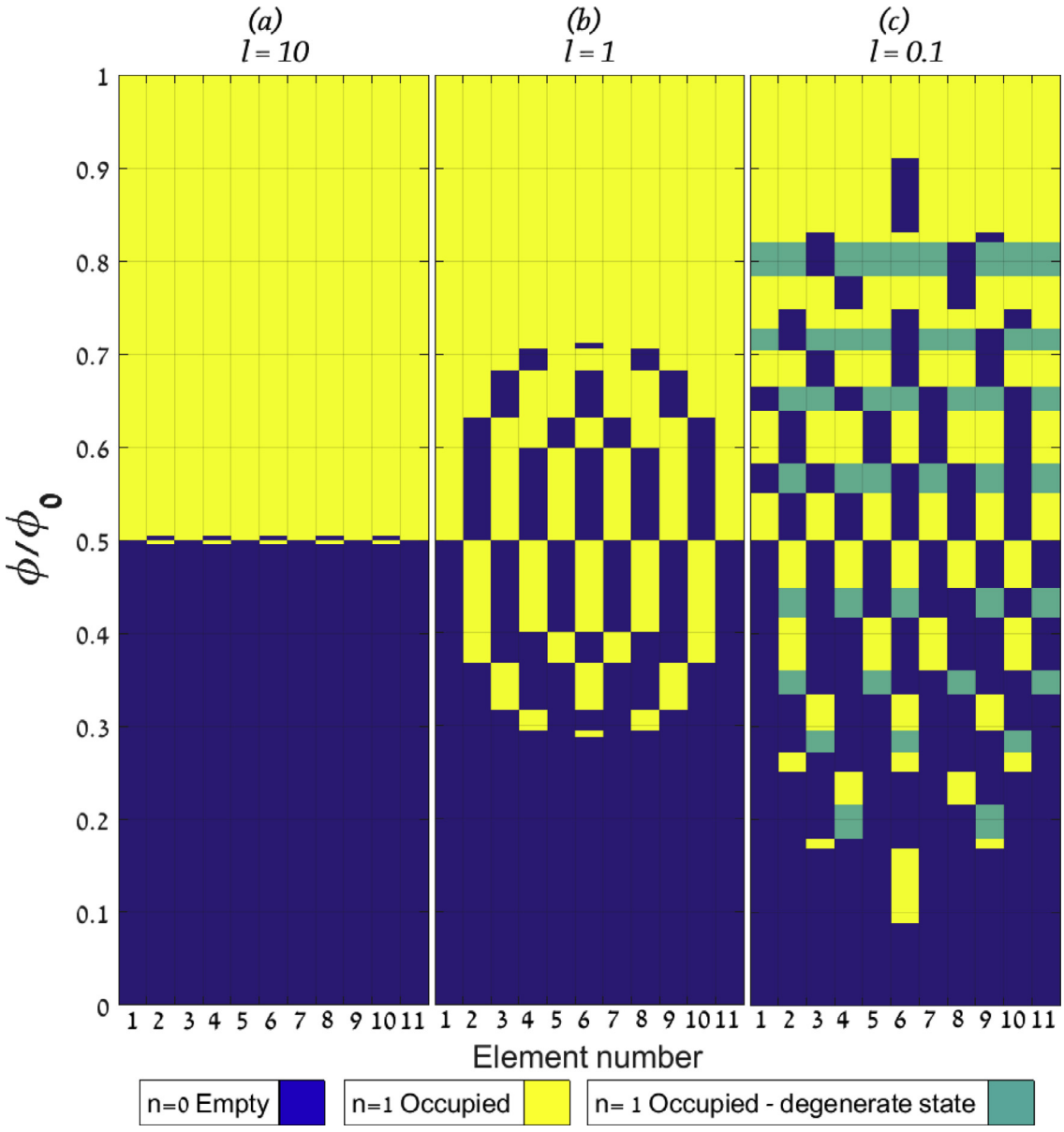

Fig. 4. Fluxoid configuration as a function of field in ladders with 11 loops, and different ratio $l = 0.1,\ 1$ and 10, between the loop length and the common width of adjacent loops. An empty loop is colored blue, and occupied loop is colored yellow or green. The green color indicates degenerated configurations which are incommensurate with the symmetry of the ladder. (For interpretation of the references to color in this figure legend, the reader is referred to the web version of this article.)

determined by the coefficients B_{ii}, is maximum at the ladder's center and drops towards the ladder's edges.

To examine the role of the self-energy in determining the fluxoids arrangements, it is useful to isolate its contribution to the total energy E. Exploiting the symmetry of $\hat{B}$, the energy E can be written in terms of the diagonal and the lower off-diagonal elements of $\hat{B}$ as follows:

$$E = \sum_{i=1}^{N} B_{ii} n_i^2 + 2\sum_{i=1}^{N-1}\sum_{j=i+1}^{N} B_{ij} n_i n_j - 2\frac{\phi}{\phi_0}\left[\sum_{i=1}^{N} B_{ii} n_i + \sum_{i=1}^{N-1}\sum_{j=i+1}^{N} B_{ij}\left(n_i + n_j\right)\right]. \quad (13)$$

The first term on the right hand side of Eq. (13) represents the self-interactions of the fluxoids, the second term represents the mutual interactions between fluxoids, and the third term expresses the interaction between the fluxoids and the effective magnetic field. Suppose that a single fluxoid enters the system at a location i_0. To minimize the energy, the location i_0 is determined by a competition between the self-interaction which prefers location at the ladder edges and the interaction with the field which favors location at the ladder's center. Explicitly, the self-interaction is $\frac{i_0(N+1-i_0)}{N+1}$, and the interaction with the field is

$$-2\frac{\phi}{\phi_0}\left[B_{i_0 i_0} + \sum_{j=i_0+1}^{N} B_{i_0 j} + \sum_{i=1}^{i_0-1} B_{i i_0}\right] = -\frac{\phi}{\phi_0} i_0 (N+1-i_0).$$

The total energy becomes:

$$i_0(N+1-i_0)\left(\frac{1}{N+1} - \frac{\phi}{\phi_0}\right).$$

From this expression it is clear that the self-interaction prevails only if $\phi < \phi_0/(N+1)$. However, in this case the entry of the first fluxoid would increase the energy of the system. A decrease

in the energy requires that $\phi > \phi_0/(N+1)$. Thus, the interaction with the field always prevails, and the first fluxoid appears at the ladder center as in the previous case. Nevertheless, the location dependent self-interaction and the stronger interaction between fluxoids, when $l \ll 1$, give rise to different fluxoid arrangements at higher fields, when more than one fluxoid occupies the ladder. In particular, a larger number of fluxoid configurations are obtained, including different configurations of the same number of fluxoids at different fields. In addition, one obtains degenerated configurations that are incommensurate to the ladder symmetry. These are demonstrated with examples in the following section.

3. Simulations

The simulations described in this section demonstrate the different configurations of fluxoids in ladders with weak, medium and strong coupling between the loops. In each case, the energy of the ladder as a function of the loops vorticities and the external field was calculated using Eq. (7) and the exact expression for the elements B_{ij} (Eq. (8)). For each given field the fluxoid arrangement $(n_1,\ n_2,\ \ldots, n_N)$ which minimizes the energy was determined.

The dashed curve in Fig. 3 shows the minimum energy as a function of the normalized flux ϕ/ϕ_0 in a ladder of 11 elements with $l = 10$. This curve exhibits the well-known Little-Parks parabolas of a single loop [2], demonstrating that the loops are essentially decoupled. A diagram of the occupation *vs.* ϕ/ϕ_0 in the first period is shown in Fig. 4a. It demonstrates that, except for a narrow region near $\phi/\phi_0 = \frac{1}{2}$, all the loops are either empty or occupied with a single fluxoid.

A different picture is obtained when l is reduced to the order of 1. The minimum energy as a function of ϕ/ϕ_0 in the case $l = 1$ is shown by the dotted curve in Fig. 3. Due to the coupling between the loops, the waveform of E *vs.* ϕ is remarkably changed, showing a broad peak around $\phi_0/2$ and crests at fluxes corresponding to fluxoid entries. The fluxoids arrangements as a function of field is illustrated in Fig. 4b. The first fluxoid enters the sixth loop at the ladder's center at $\phi/\phi_0 = 0.29$. As the field increases a second fluxoid enters ladder, pushing the first one out of its central position and both fluxoids arrange themselves symmetrically in the fourth and eighth loops, keeping apart from each other and away from the network edges. As more fluxoids enter the ladder with increasing field, rearrangement of fluxoids continues until the last fluxoid enters the ladder's center completing one period in which each loop is occupied with one fluxoid. Occupation of the loops in the following periods follows the same pattern.

When l decreases much below 1, the coupling between the loops increases significantly giving rise to a more complex E *vs.* ϕ curve, as shown by the solid line in Fig. 3 for $l = 0.1$. The additional crests in the $E(\phi)$ curve indicate additional configurations of fluxoids through a period as illustrated in Fig. 4c. It is interesting to note that some of these configurations are incommensurate to the ladder symmetry (marked in green color in Fig. 4c). The first fluxoid enters the ladder's center, as in the previous case. However, with the entry of the second fluxoid, both arrange themselves farther away from each other, in the third and 9th loops, closer to the ladder's edges. With increasing field, both fluxoids rearrange themselves in asymmetric positions, in the fourth and 9th loops. This configuration is degenerated in energy with a configuration where the third and 8th loops are occupied. Rearrangements from symmetric to asymmetric positions also occurs with three and five fluxoids, as shown in Fig. 4c. A 'checkerboard' arrangement is obtained with 5 and 6 fluxoids around $\phi_0/2$. The configurations of 7, 8, 9, 10 and 11 fluxoids are complementary to the configurations of the 4, 3, 2, 1 and zero fluxoids, respectively.

Our analysis of superconducting ladders can be extended to two dimensional superconducting networks. However, the interaction terms between fluxoids, and between them and the external field, become more complicated. In a recent publication [27] we showed numerical results for a 3×3 square network, based on the J^2 model. These numerical-calculations yield 11 different configurations, exceeding the number of loops in the network, due to rearrangement of the same number of fluxoids as the field increases. Among the 11 different configurations, there are 6 degenerated states that are incommensurate to the network symmetry. Calculations of Kato and Sato based on the de-Gennes-Alexander equations for a network yield quite different results [17]. Involving the appearance of anti-fluxoids in the network, their calculations predict 9 configurations all of which are commensurate to the network symmetry. It should be noted, however, that by minimizing the Ginzburg–Landau free energy, asymmetric fluxoid patterns have been reported for a 10×10 network [28]. Experimental work, using, e.g., a scanning SQUID-on-tip [29,30], is required to decide between the predictions of the J^2- and de-Gennes-Alexander models.

4. Summary and conclusions

The fluxoids equilibrium positions in ladders consisting of rectangular loops depend on the ratio l between the loops length and the common width of adjacent loops. For $l \gg 1$ the interaction between fluxoids is weak and, in essence, they occupy the ladder's loops independently as if the loops are decoupled. In ladders with $l \gtrsim 1$, a 'short range' repulsive interactions between fluxoids arise, which decreases exponentially with their relative separation. The fluxoids arrangement is dictated by a competition between their repulsive interaction and their interaction with the external magnetic field which drives them toward the ladder's center. Ladders with $l << 1$ are characterized by a 'long range' interaction between fluxoids, which depends on the product of their locations relative to the ladder's edges. In the competition between this long range interaction and the interaction with the field another factor plays a role, namely the fluxoids self-interaction. Consequently, in such ladders, different fluxoids configurations are obtained. In particular, additional configurations are obtained extending over a wider range of magnetic flux. Some of these configurations include the same number of fluxoids arranged in different positions, some of which are incommensurate to the ladder symmetry.

Finally we note that the basic mechanism governing the fluxoid arrangements in ladders should also apply to two dimensional networks. However, a full extension of our analysis to two dimensional networks remains for a future study. The results of this study could connect to many theoretical and experimental works on films with antidot arrays, which become networks in the limit of large antidots, see e.g. [31].

Acknowledgments

This work was partially supported by the German-Israeli Foundation (GIF - Grant No. I-1234-303.10/2014). A.S. acknowledges a financial support from the Israel Science Foundation (ISF - Grant No. 164/12).

References

[1] A.O. Caldeira, An Introduction to Macroscopic Quantum Phenomena and Quantum Dissipation, Cambridge University Press, 2014.
[2] M. Tinkham, Introduction to Superconductivity, McGraw-Hill, Inc., 1996.
[3] B. Pannetier, J. Chaussy, R. Rammal, Experimental determination of the (H, T) phase diagram of a superconducting network, Journal de Physique Lettres 44 (1983) 853–858.
[4] B. Pannetier, J. Chaussy, R. Rammal, J. Villegier, Experimental fine tuning of frustration: two-dimensional superconducting network in a magnetic field, Phys. Rev. Lett. 53 (1984) 1845.

[5] J.M. Gordon, A.M. Goldman, J. Maps, D. Costello, R. Tiberio, B. Whitehead, Superconducting-normal phase boundary of a fractal network in a magnetic field, Phys. Rev. Lett. 56 (1986) 2280.
[6] A. Behrooz, M. Burns, D. Levine, B. Whitehead, P. Chaikin, Superconducting phase boundary of aperiodic networks in a magnetic field, Phys. Rev. B 35 (1987) 8396.
[7] J.M. Gordon, A.M. Goldman, B. Whitehead, Dimensionality crossover in superconducting wire networks, Phys. Rev. Lett. 59 (1987) 2311.
[8] F. Nori, Q. Niu, Tc (H) for quasicrystalline micronetworks: Analytical and numerical results, Physica B 152 (1988) 105–112.
[9] C. Chi, P. Santhanam, P. Blöchl, Interacting loop-current model of superconducting networks, J. Low Temp. Phys. 88 (1992) 163–195.
[10] V. Bruyndoncx, C. Strunk, V. Moshchalkov, C. Van Haesendonck, Y. Bruynseraede, Fluxoid quantization effects in superconducting mesoscopic Al multiloop structures, EPL 36 (1996) 449.
[11] D.H. Reich, D.M. Silevitch, C. Chien, D. Davidovic, S. Field, Disorder and correlations in extended superconducting nanostructures, J. Alloys Compounds 303 (2000) 245–251.
[12] A. Burlakov, V. Gurtovoĭ, S. Dubonos, A.V. Nikulov, V. Tulin, Little-parks effect in a system of asymmetric superconducting rings, JETP Lett. 86 (2007) 517–521.
[13] I. Sochnikov, A. Shaulov, Y. Yeshurun, G. Logvenov, I. Božović, Large oscillations of the magnetoresistance in nanopatterned high-temperature superconducting films, Nature Nanotechnol. 5 (2010) 516–519.
[14] I. Sochnikov, A. Shaulov, Y. Yeshurun, G. Logvenov, I. Božović, Oscillatory magnetoresistance in nanopatterned superconducting La 1.84 Sr 0.16 CuO 4 films, Phys. Rev. B 82 (2010) 094513.
[15] I. Sochnikov, I. Božović, A. Shaulov, Y. Yeshurun, Uncorrelated behavior of fluxoids in superconducting double networks, Phys. Rev. B 84 (2011) 094530.
[16] G. Berdiyorov, M. Milošević, M. Latimer, Z. Xiao, W. Kwok, F. Peeters, Large magnetoresistance oscillations in mesoscopic superconductors due to current-excited moving vortices, Phys. Rev. Lett. 109 (2012) 057004.
[17] M. Kato, O. Sato, Magnetic flux structures of finite superconducting networks, Supercond. Sci. Technol. 26 (2013) 033001.
[18] M. Itzler, A. Behrooz, C. Wilks, R. Bojko, P. Chaikin, Commensurate states in disordered networks, Phys. Rev. B 42 (1990) 8319.
[19] C. Reichhardt, C.O. Reichhardt, A Bishop, Commensurate and incommensurate checkerboard charge ordered states, Physica C 460 (2007) 1178–1179.
[20] O.V. Dobrovolskiy, Abrikosov fluxonics in washboard nanolandscapes, Physica C (2016).
[21] R. Gross, A. Marx, D. Einzel, From flux quantization to superconducting quantum bits, J. Superconduct. Novel Magnet. 19 (2006) 331–340.
[22] M.V. Milošević, G.R. Berdiyorov, F.M. Peeters, Fluxonic cellular automata, Appl. Phys. Lett. 91 (2007) 212501.
[23] M. Milošević, F. Peeters, Vortex manipulation in a superconducting matrix with view on applications, Appl. Phys. Lett. 96 (2010) 192501.
[24] P. Chaikin, A. Behrooz, M. Itzler, C. Wilks, B. Whitehead, G. Grest, D. Levine, Studies of quasicrystalline superconducting networks, Physica B 152 (1988) 113–124.
[25] R.T. Giles, F.V. Kusmartsev, Critical fields and devil's staircase in superconducting ladders, Physica B 284 (2000) 1850–1851.
[26] C. Da Fonseca, J. Petronilho, Explicit inverse of a tridiagonal k– Toeplitz matrix, Numerische Mathematik 100 (2005) 457–482.
[27] O.J. Sharon, N. Haham, S. Avner, Y. Yeshurun, Fluxoids behavior in superconducting ladders, in: IOP Conference Series, Proceedings of LT28, Gothenburg, Sweden, 2017.
[28] M. Hayashi, H. Ebisawa, M. Kato, Vortex structures in mesoscopic superconducting network systems, Physica C 426 (2005) 136–140.
[29] D. Vasyukov, Y. Anahory, L. Embon, D. Halbertal, J. Cuppens, L. Neeman, A. Finkler, Y. Segev, Y. Myasoedov, M.L. Rappaport, A scanning superconducting quantum interference device with single electron spin sensitivity, Nature Nanotechnol. 8 (2013) 639–644.
[30] Y. Anahory, J. Reiner, L. Embon, D. Halbertal, A. Yakovenko, Y. Myasoedov, M.L. Rappaport, M.E. Huber, E. Zeldov, Three-junction SQUID-on-tip with tunable in-plane and out-of-plane magnetic field sensitivity, Nano Lett. 14 (2014) 6481–6487.
[31] G. Berdiyorov, M. Milošević, F. Peeters, Vortex configurations and critical parameters in superconducting thin films containing antidot arrays: nonlinear Ginzburg–Landau theory, Phys. Rev. B 74 (2006) 174512.